ACS APPLIED MATERIALS & INTERFACES

Research Article

www.acsami.org

Enhanced Cycle Performance of Lithium–Sulfur Batteries Using a Separator Modified with a PVDF-C Layer

Hang Wei, Jin Ma, Biao Li, Yuxuan Zuo, and Dingguo Xia*

College of Engineering, Peking University, Beijing 100871, P. R. China

Supporting Information

ABSTRACT: High energy density Li–S batteries are highly attractive. However, their use in practical applications has been greatly affected by their poor cycle life and low rate performance, which can be partly attributed to the dissolution of polysulfides from the S cathode and their migration to the Li anode through the separator. While much effort has been devoted to designing the structure of the S cathodes for suppressing the dissolution of polysulfides, relatively little emphasis has been placed on modifying the separator. Herein, we demonstrate a new approach for modifying the separator with a polyvinylidene fluoride-carbon (PVDF-C) layer, where the polysulfides generated in the Li–S cells can be localized on the cathode side. Li–S batteries based on the novel separator and a cathode prepared by the simple mixing of a S powder and super P have delivered discharge capacities of 918.6 mAh g^{-1}, 827.2 mAh g^{-1}, and 669.1 mAh g^{-1} after 100, 200, and 500 cycles, respectively, at a discharge rate of 0.5 C. Even under current densities of up to 5 C, the cells were able to retain a discharge capacity of 393 mAh g^{-1}, thereby demonstrating an excellent high rate performance and stability. The exceptional electrochemical performance could be attributed to the intense adsorption capability of the micropores, presence of C–C double bonds, and conductivity of the C network in the PVDF-C layer. This economical and simple strategy to overcome the polysulfide dissolution issues provides a commercially feasible method for the construction of Li–S batteries.

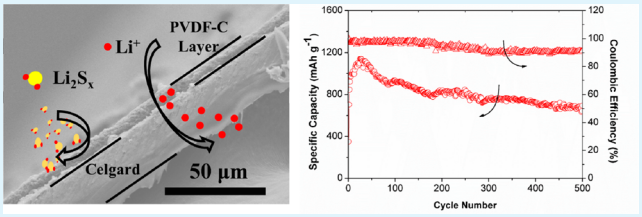

KEYWORDS: *high-performance lithium sulfur battery, PVDF-C layer, modified separator*

INTRODUCTION

The rapid development of portable electronics, electric vehicles, and energy storage devices has triggered enormous research efforts toward developing next-generation rechargeable batteries with high energy densities.[1−3] Among all the rechargeable batteries available, the Li–S cell is one of the most promising candidates due to its extremely high discharge specific capacity of 1675 mAh g^{-1}, low cost, and environmentally benign and facile processing.[4−8] However, several drawbacks such as poor cycle life and low rate performance have hindered the practical application of Li–S batteries.[9−11] The main reasons for the poor cycle life and the low rate performance are the low conductivity of S and the shuttle phenomenon of polysulfides during charge–discharge, leading to poor active material utilization and rapidly declining capacity.[12]

In order to overcome these problems, tremendous efforts have been made toward improving the electrochemical performance of Li–S cells by modifying the S cathode, including the immobilization of S in porous conducting composites through weak intermolecular interactions[13−19] and physically encapsulating the S particles in hollow spherical structures.[20−25] While these approaches have shown a significant enhancement in the electrochemical performance of Li–S batteries, the material processing steps are often elaborate and the loading of the active mass is usually very low, limiting the feasibility of manufacturing a viable Li–S cell. Recently, several studies have demonstrated a promising strategy for improving the rate capability and cycle life of Li–S batteries by the insertion of an interlayer.[26−30] While on the one hand, the conductive interlayer can reduce the charge transfer resistance of the S cathodes, on the other hand, the interlayer can localize and retain the dissolved active material during cycling. This strategy leads to enhanced cycle stability. However, the insertion of a thick interlayer is not favorable for enhancing the energy density of the Li–S batteries.

The separator, which is an indispensable part of the battery, has been usually studied in the context of improving the high-temperature performance and safety properties of the cells.[31,32] In Li–S batteries, it is noteworthy that the shuttle effect occurs by the passage of polysulfide ions through the separator. As a result, modification of the separator by using other chemicals may be a convenient and an efficient approach to localize the polysulfides on the cathode side and prevent them from shuttling between the cathode and the anode. It is well-known that polyvinylidene fluoride (PVDF) is not only one of the most widely used materials for commercial binders in Li-ion batteries[33,34] but also is the most common material used for microfiltration membranes due to its superior bonding ability, chemical resistance, great stability, and high mechanical strength.[32,35,36] In view of its advantages, in the present work,

Received: August 27, 2014
Accepted: October 2, 2014
Published: October 2, 2014

we report a facile and effective method for suppressing the shuttle effect in Li−S batteries by using a separator modified with a thin PVDF-C layer, produced by using the phase-inversion process. The PVDF-C layer is designed with a reticular microporous structure, which may act both as an electron pathway as well as a trap for dissolved polysulfides.

EXPERIMENTAL SECTION

Materials. PVDF powders were obtained from Solvay and Super P was from WILLEBROEK-BELGIUM. Sublimed sulfur, $NH_3{\bullet}H_2O$, KOH, and all other used reagents were all purchased from Sinopharm Chemical Reagent Beijing Co. Ltd. All chemical reagents were of analytical grade and were used as purchased without any further purification.

Sample Preparation. A schematic illustration of the preparation of a PVDF-C-modified separator is shown in Scheme 1. A PVDF-C

Scheme 1. Schematic Illustration of the Formation of the PVDF-C-Modified Separator via a Phase-Inversion Process

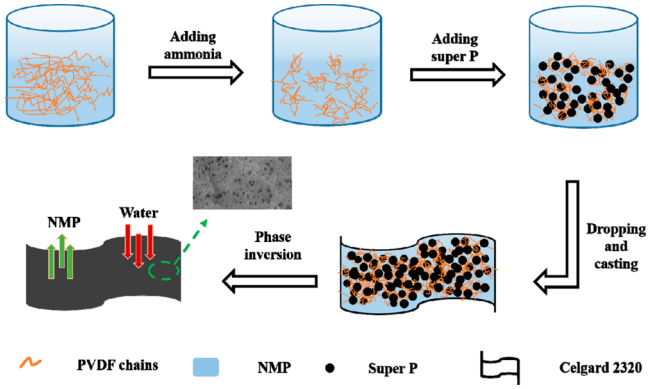

mixed solution was prepared using a simple mixing process. The PVDF powder (0.5 g) was dissolved in 10 mL of NMP under stirring to form a transparent solution. Aqueous ammonia (28%, 500 μL) was added to the above solution to form a transparent sol. KOH-activated super P (0.15 g) was then added, and the mixture was stirred for 6 h to obtain a black sol. A certain amount of the sol containing Super P was applied and cast onto Celgard 2320, which was used as the substrate. Finally, the separator modified with the PVDF-C layer was obtained using a phase-inversion process, in which the Celgard 2320 separator coated with the sol containing Super P was immersed in water and KOH solutions to remove NMP and promote the formation of C−C double bonds, respectively. The resulting PVDF-C-modified separator was rinsed in deionized water several times and dried in an oven at 60 °C for 12 h. The weight of PVDF-C layer is about 0.068 mg cm^{-2}. Besides, PVDF-modified separator was prepared in the same way in the absence of Super P for the comparison.

Characterization. The morphology of the PVDF-C-modified separator was characterized using a Hitachi S-4800 high resolution scanning electron microscope (SEM) operated at 10 kV. The BET analysis was performed on the PVDF-C membrane peeled off from the substrate using the nitrogen adsorption technique with a Micromeritrics ASAP 2010 accelerated surface area and porosimetry analyzer after degassing the sample for 12 h at 60 °C. Fourier transform infrared-attenuated total reflectance (FTIR-ATR) spectra of the pristine and PVDF-C-modified separators were measured on a Nicolet ECTOR22 spectrometer. The contact angles and X-ray diffraction (XRD) patterns of the separators were recorded using a Nikon D7100 SLR camera and a Bruker D8 Advance X-ray diffractometer using filtered Cu Kα (λ = 1.5405 Å) radiation, respectively.

Electrochemical Measurements. The cathode was prepared by the vigorous mixing of elemental sulfur (S), super P, and the polytetrafluoroethylene (PTFE) binder in a 7:2:1 mass ratio, with a small amount of isopropyl alcohol, followed by roll-compressing and cutting into regular film sheets. The loading of S in the cathode is about 7 mg cm^{-2}. A composite cathode consisting of reduced graphene oxide and multiwalled carbon nanotubes containing S (RGO/MWCNTs/S) was also prepared according to Zhou's report.[37] Prior to assembling the cells for testing, the film sheets were dried in a vacuum oven at 60 °C for 12 h. CR2032 coin cells were then assembled in a glovebox filled with Ar. Li metal was used as the anode, and a mixture of 1,3-dioxolane (DOL) and 1,2-dimethoxyethane (DME) (in a 1:1 volume ratio) along with 1 M lithium bis(trifluoromethanesulfonyl)imide (LiTFSI) and 0.1 M $LiNO_3$ was used as the electrolyte. Pristine Celgard 2320 and PVDF-C-modified Celgard 2320 were used as the separators. The cells were charged and discharged at various current densities in the voltage range 1.7−2.8 V using a Neware multichannel battery tester at room temperature. The cyclic voltammetry (CV) and electrochemical impedance spectroscopy (EIS) measurements were conducted on an SP-240 workstation (Bio-Logic Science Instruments, France). The frequency range was varied from 100.0 kHz to 10 mHz with an AC signal amplitude of 5 mV.

RESULTS AND DISCUSSION

Figure 1a shows the top surface morphology of the PVDF-C-modified separator. It can be seen that the PVDF-C layer

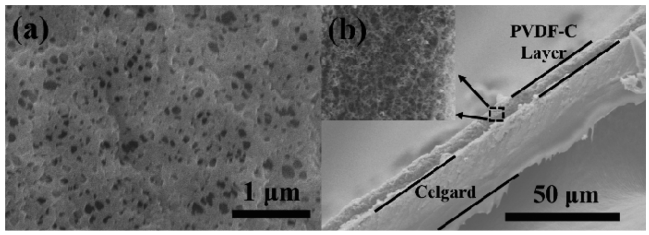

Figure 1. SEM images (a) of the top surface and (b) a typical side-view of the PVDF-C-modified separator.

showed a uniformly reticular porous structure without any visible agglomeration of C. Figure 1b and the inset present cross-sectional images of the modified separator. As shown in the SEM images, the PVDF-C porous layer was stacked well on the surface of the separator and was ~5 μm thick on average.

A comparison of the nitrogen adsorption/desorption isotherms of the PVDF-C layer with those of the pristine separator is shown in Figures 2a. Both the PVDF-C layer and the pristine separator showed type IV isotherms, indicating the existence of mesopores. However, the PVDF-C layer has more micropores with a diameter of less than 10 nm, indicating that the PVDF-C-modified separator was similar to a typical nanofiltration separator, while the pristine separator showed more pores with about 100 nm, as shown in Figure 2b. Figure 2c illustrates a proposed mechanism of dehydrofluorination of PVDF in the presence of an alkaline solution. The chemical attack of the alkali onto PVDF induces a dehydrofluorination of the polymer structure.[38,39] Figure 2d, which plots the IR spectrum of the PVDF-C layer and Celagrd 2320, has shown the huge difference between them. The IR specrum of Celgard 2320 just reflects the characteristic of polypropylene. The peaks at 1454 and 1372 cm^{-1} are assigned to the CH_3 symmetric stretching behavior, and the other tiny bands are assigned variously to CH_3, CH, CH, CCH_3, and CH_2 vibrations.[40] However, the PVDF consisted of a "$-CH_2-CF_2-$" molecular chain is highly flexible and gives some stereochemical constraint. The main crystalline forms of PVDF can be distinguished from the FTIR spectrum due to its distinct molecular conformations. From Figure 2d, the unit cell of PVDF demonstrates form I crystalline form, which contains

dx.doi.org/10.1021/am505807k | ACS Appl. Mater. Interfaces 2014, 6, 20276−20281

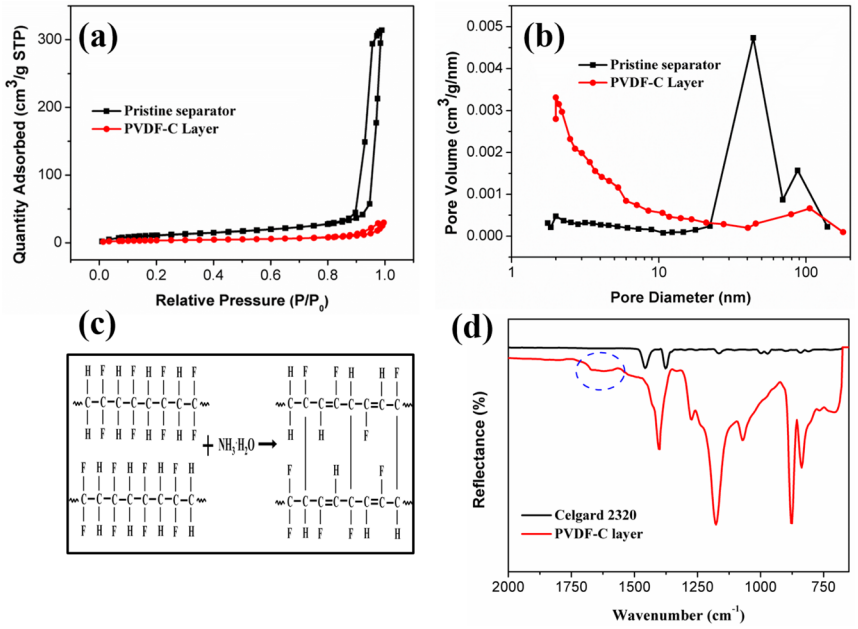

Figure 2. (a) Nitrogen adsorption/desorption isotherms and (b) pore size distribution of the PVDF-C layer and pristine separator, (c) proposed mechanism of dehydrofluorination in PVDF, and (d) FTIR-ATR spectrum of the PVDF-C layer and pristine separator.

polymer chains with an all trans structure.[41] The 1401 and 837 cm^{-1} peak are assigned to the CH_2 deformation rocking vibration, and the 1274 and 1071 cm^{-1} are contributed by the CF deformation vibration. In addition, 1180 and 878 cm^{-1} are assigned to the C−C skeleton stretching vibration.[42] Most importantly, a new broad absorption band appears at around 1630 cm^{-1}, which is assigned to the stretching bands of the C−C double bonds.[43−45] The C−C double bonds can promote the binding of S to the C−C bonds, resulting in the adsorption of polysulfides. Considering the intense adsorption capability of the micropores, existence of C−C double bonds, and conductivity of the C network, it is clear that the unique network in the PVDF-C layer is not only capable of capturing polysulfides and suppressing its migration to the Li anode but can also promote the electron transfer of the S cathode.

The surface composition and chemistry of the separator also play an important role in the diffusion of the polysulfides due to the interaction between the polysulfides and the separator. In contrast to the IR spectrum of the unmodified separator (Figure 2d), the PVDF-C layer showed an increase in the percentage of area occupied by oxygen-containing groups because of the addition of Super P, which may enhance the hydrophilicity of the separator. The contact angle measurements were conducted to confirm the increase in the surface hydrophilicity of the separator modified with the PVDF-C layer.[46,47] As expected, Figure 3 shows that the PVDF-C layer had a lower contact angle than the unmodified separator, indicating that the PVDF-C layer was more hydrophilic than the unmodified separator. Owing to the strong hydrophilicity of the polysulfides, the enhanced hydrophilicity of the PVDF-C-modified separator will be beneficial in suppressing the shuttle effect by the adsorption of the polysulfides on the separator.[27,30]

The electrochemical performances of the Li−S batteries containing the separator modified with PVDF-C and the pristine separator were evaluated by cyclic voltammetry (CV) and galvanostatic charge/discharge cycling. As shown in Figure 4a, for a battery containing the pristine separator, the cathodic

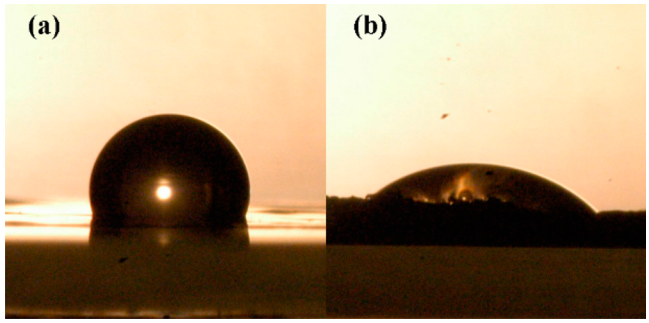

Figure 3. Contact angle of water on (a) the pristine separator and (b) the PVDF-C layer.

peaks vanished on increasing the number of CV cycles, indicating that the electrochemical activity of the electrode was completely inhibited due to the intense shuttle effect of the polysulfides. On the other hand, the CV curves for the battery with the separator modified by the PVDF-C layer (Figure 4b) exhibited two cathodic peaks at around 2.23 and 1.93 V vs Li/Li^+, which were assigned to the transformation from S_8 to Li_2S_4 and Li_2S_4 to insoluble Li_2S_2 or Li_2S, respectively; and a broad anodic peak at around 2.4 V vs Li/Li^+ indicated the typical elemental sulfur converting process. Importantly, the position and shape of the anodic and cathodic peaks obtained during different CV cycles were almost similar, indicating the high reversibility of the chemical reactions of the cell containing a PVDF-C-modified separator.[17,24]

Typical charge/discharge profiles obtained in a voltage window of 1.7−2.8 V vs Li/Li+ are shown in Figure 5. The batteries containing the PVDF-C-modified separator delivered a specific capacity of 1150 mAh g^{-1} after the first 20 discharge cycles at a current density of 0.5 C and exhibited two discharge plateaus. The capacities were calculated based on the mass of S. A much improved cycling stability was achieved for the battery containing the PVDF-C-modified separator compared to the battery containing the unmodified separator. Even after 100,

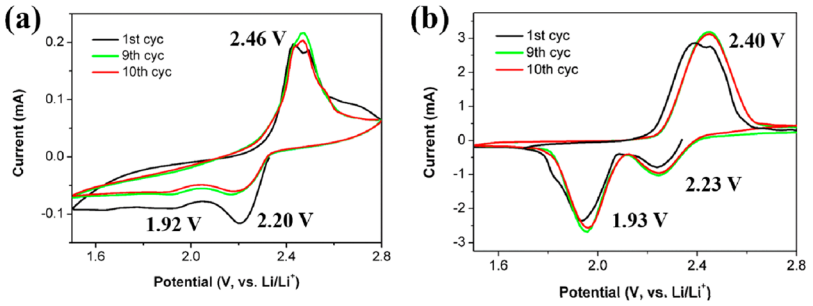

Figure 4. Cyclic voltammogram scans of Li−S cells with (a) the pristine separator (b) and the PVDF-C-modified separator (both of scan rate are 0.1 mV s^{-1}).

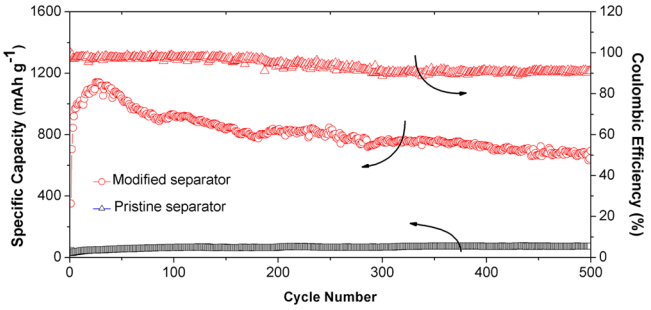

Figure 5. Discharge capacities and Coulombic efficiency vs the cycle number of Li−S cells with pristine and modified separators at a current density of 0.5 C.

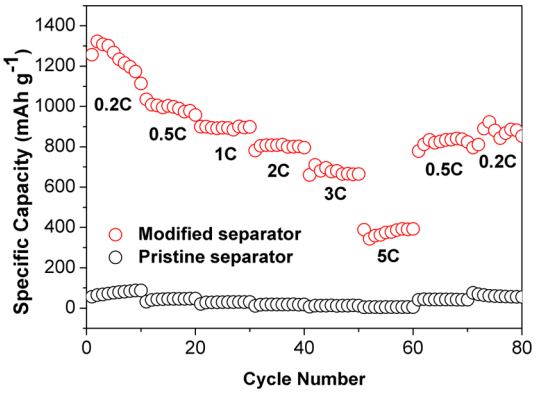

Figure 6. Discharge capacities of Li−S cells with pristine and PVDF-C-modified separators at different current densities.

200, and 500 cycles, discharge capacities of 918 mAh g^{-1}, 827 mAh g^{-1}, and 669 mAh g^{-1}, respectively, were achieved with a Coulombic efficiency of more than 90%. When the unmodified separator was used, an initial discharge capacity of 42.6 mAh g^{-1} was observed at the current density of 0.5 C, and the capacity did not exceed 80 mAh g^{-1} in the hundreds of cycles that followed. This result implies that the introduction of the PVDF-C layer can effectively prevent the diffusion of the polysulfide anions through the separator, thereby inhibiting the reactions between the polysulfides and the Li anode. Interestingly, to demonstrate the necessity of carbon additive, the performance of the PVDF coating layer in the absence of carbon was shown in Figure S1. The results show the capacity of cell with only PVDF modified separator decays fast and is just 487 mAh g^{-1} after 100 cycles at 0.5 C. This is because PVDF-C layer not only can suppress the shuttle effect but also improve the conductivity of lithium-ion batteries and reduce the charge transfer resistance. On the contrast, PVDF is a nonconductive material. In addition, the KOH activated carbon has strong hydrophilic properties, which is more beneficial for the adsorption of polysulfide ion.

A significant improvement was also achieved in the rate capability of the batteries by using the PVDF-C-modified separator as opposed to the pristine separator. As shown in Figure 6, the cells containing the PVDF-C-modified separator showed a much higher capacity than those containing the pristine separator under all current densities that were investigated. Even under the very high current density of 5 C, the cell containing the PVDF-C-modified separator still exhibited a favorable specific capacity of 339 mAh g^{-1} after 60 cycles, while the cell with the pristine separator showed a specific capacity value below 10 mAh g^{-1}. Importantly, after the high rate measurements, the specific capacities of the cells cycled at the current density of 5 C returned to their initial values, implying good reversibility.

The enhanced electrical conductivity of the PVDF-C-modified separator was confirmed using electrochemical impedance spectroscopy (EIS). Figure 7 compares the Nyquist

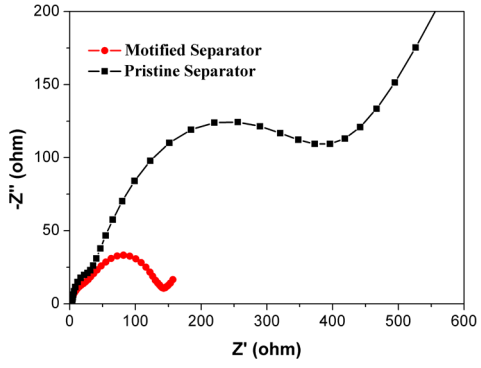

Figure 7. Electrochemical impedance spectra of Li−S cells with pristine and PVDF-C-modified separators.

plots for the PVDF-C-modified and pristine separators. The PVDF-C-modified separator showed a much lower charge transfer resistance (R_{ct}) than the pristine separator. This result indicates that the PVDF-C layer exhibits a high electrical conductivity, resulting in a better rate capability and a higher reversible capacity than the pristine separator, similar to the phenomenon found in other works using interplay.[23,26,48]

In order to further validate the excellent performance of the Li−S cells containing the PVDF-C-modified separators, an RGO/MWCNT/S composite was also synthesized according

to Zhou's report.[37] Figure S2a shows the XRD pattern of the RGO/MWCNT/S composite. After wrapped into the RGO/MWCNT matrix, the diffraction peaks of S became less noticeable compared to the orthorhombic structure of crystalline state S, demonstrating that the sulfur existed in a highly dispersed state. Figure S2b exhibits the electrochemical behavior of a Li−S cell where the RGO/MWCNT/S composite was used as the cathode along with a PVDF-C-modified separator. After the initial activation cycles, a discharge capacity of up to 1231 mAh g^{-1} was achieved at a discharge current density of 1 C, and the discharge capacities remained at 1201 mAh g^{-1} and 992 mAh g^{-1} at discharge current densities of 2 and 3 C, respectively. Even when the cell was cycled at 5 C, the discharge capacity was still retained at 788 mAh g^{-1}. After cycling at various rates, when the current density was returned to 1 C, the cell capacity returned to a stable value of 1055 mAh g^{-1}, which was close to the initial value obtained during the initial cycles. These results further reveal the unique and outstanding performance of the PVDF-C-modified separator when used in the Li−S cells.

Figure 8a,b shows the SEM and EDS results obtained for the cycled cell components, respectively, which further aids in understanding the mechanism of the PVDF-C layer when used in Li−S cells. The SEM image of the PVDF-C layer exhibited a glue-like network morphology, and the surface became smooth after 100 cycles at 0.2 C, implying that the migrating active polysulfides might be adsorbed and captured during the electrochemical cycling.[30] The elemental mapping results of the PVDF-C layer toward the cathode after cycling showed that a homogeneously distributed S signal was found all over the modified layer. This further confirms the trapping of polysulfide within the PVDF-C layer.

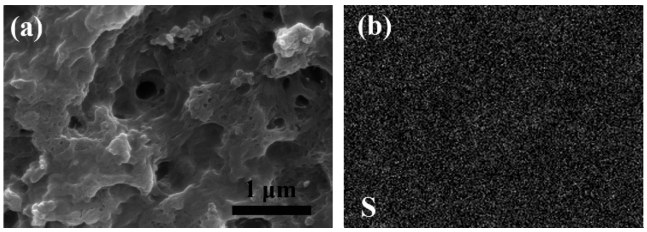

Figure 8. (a) SEM image of the PVDF-C-modified separator (toward the cathode side) and (b) elemental mapping of S on the PVDF-C-modified separator after 100 cycles at a current density of 0.2 C.

The much improved electrochemical performance of the Li−S cells containing the PVDF-C-modified separator compared to the cells containing the pristine separator could be attributed to the unique properties of the PVDF-C layer modification. In this work, pure S powder was employed as the active material, and the cathode was loaded with approximately 7 mg cm^{-2} of S. It may be noted that we did not use any specialized composites or introduce any other surface modifications on the conventional S cathodes. Therefore, the observed improvements in cyclability arises solely from the modifications made to the separator by incorporating a PVDF-C layer.

CONCLUSIONS

In summary, a novel separator modified with a PVDF-C layer was fabricated using a phase inversion process. The resultant Li−S battery cell showed a prolonged cycling capability, with discharge capacities of 918 mAh g^{-1}, 827 mAh g^{-1}, and 669 mAh g^{-1} recorded after 100, 200, and 500 cycles, respectively, when discharged at a current density of 0.5 C. The improved cycling stability and long cycle performance of the cells are attributed to the intense adsorption capability of the micropores, presence of the C−C double bonds, and conductivity of C network in the PVDF-C layer. The PVDF-C layer can not only localize the polysulfides on the cathode side but can also enhance the conductivity of the electrode. Considering the safe and simple fabrication process, this approach offers a general strategy that can be utilized in the future designs of advanced Li−S cells.

ASSOCIATED CONTENT

Supporting Information

Figures S1 and S2. This material is available free of charge via the Internet at http://pubs.acs.org.

AUTHOR INFORMATION

Corresponding Author

*E-mail: dgxia@pku.edu.cn.

Author Contributions

The manuscript was written through contributions of all authors. All authors have given approval to the final version of the manuscript.

Notes

The authors declare no competing financial interest.

ACKNOWLEDGMENTS

This work was financially supported by the National Nature Science Foundation of China (No. 11179001), the National High Technology Research and Development Program of China (No. 2012AA052201, 2011AA11A254), and thte Program for New Century Excellent Talents in University (NCET-12-0603).

REFERENCES

(1) Liu, C.; Li, F.; Ma, L.-P.; Cheng, H.-M. Advanced Materials for Energy Storage. *Adv. Mater.* **2010**, *22*, E28−E62.

(2) Armand, M.; Tarascon, J. M. Building Better Batteries. *Nature* **2008**, *451*, 652−657.

(3) Goodenough, J. B.; Kim, Y. Challenges for Rechargeable Li Batteries. *Chem. Mater.* **2009**, *22*, 587−603.

(4) Ji, X.; Nazar, L. F. Advances in Li-S Batteries. *J. Mater. Chem.* **2010**, *20*, 9821−9826.

(5) He, G.; Hart, C. J.; Liang, X.; Garsuch, A.; Nazar, L. F. Stable Cycling of a Scalable Graphene-Encapsulated Nanocomposite for Lithium−Sulfur Batteries. *ACS Appl. Mater. Interfaces* **2014**, *6*, 10917−10923.

(6) Kim, J.; Lee, D.-J.; Jung, H.-G.; Sun, Y.-K.; Hassoun, J.; Scrosati, B. An Advanced Lithium-Sulfur Battery. *Adv. Funct. Mater.* **2013**, *23*, 1076−1080.

(7) Rao, M. M.; Geng, X. Y.; Li, X. P.; Hu, S. J.; Li, W. S. Lithium-Sulfur Cell with Combining Carbon Nanofibers−Sulfur Cathode and Gel Polymer Electrolyte. *J. Power Sources* **2012**, *212*, 179−185.

(8) Yin, L.; Wang, J.; Lin, F.; Yang, J.; Nuli, Y. Polyacrylonitrile/Graphene Composite as a Precursor to a Sulfur-Based Cathode Material for High-Rate Rechargeable Li−S Batteries. *Energy Environ. Sci.* **2012**, *5*, 6966−6972.

(9) Yamin, H.; Gorenshtein, A.; Penciner, J.; Sternberg, Y.; Peled, E. Lithium Sulfur Battery Oxidation/Reduction Mechanisms of Polysulfides in THF Solutions. *J. Electrochem. Soc.* **1988**, *135*, 1045−1048.

(10) Zheng, W.; Liu, Y.; Hu, X.; Zhang, C. Novel Nanosized Adsorbing Sulfur Composite Cathode Materials for the Advanced Secondary Lithium Batteries. *Electrochim. Acta* **2006**, *51*, 1330−1335.

(11) Mikhaylik, Y. V.; Akridge, J. R. Polysulfide Shuttle Study in the Li/S Battery System. *J. Electrochem. Soc.* **2004**, *151*, A1969−A1976.
(12) Akridge, J. R.; Mikhaylik, Y. V.; White, N. Li/S Fundamental Chemistry and Application to High-Performance Rechargeable Batteries. *Solid State Ionics* **2004**, *175*, 243−245.
(13) Ji, X.; Lee, K. T.; Nazar, L. F. A Highly Ordered Nanostructured Carbon-Sulphur Cathode for Lithium-Sulphur Batteries. *Nat. Mater.* **2009**, *8*, 500−506.
(14) Elazari, R.; Salitra, G.; Garsuch, A.; Panchenko, A.; Aurbach, D. Sulfur-Impregnated Activated Carbon Fiber Cloth as a Binder-Free Cathode for Rechargeable Li-S Batteries. *Adv. Mater.* **2011**, *23*, 5641−5644.
(15) Chen, J.-j.; Zhang, Q.; Shi, Y.-n.; Qin, L.-l.; Cao, Y.; Zheng, M.-s.; Dong, Q.-f. A Hierarchical Architecture S/MWCNT Nanomicrosphere with Large Pores for Lithium Sulfur Batteries. *Phys. Chem. Chem. Phys.* **2012**, *14*, 5376−5382.
(16) Huang, J.-Q.; Zhang, Q.; Zhang, S.-M.; Liu, X.-F.; Zhu, W.; Qian, W.-Z.; Wei, F. Aligned Sulfur-Coated Carbon Nanotubes with a Polyethylene Glycol Barrier at one end for use as a high efficiency Sulfur Cathode. *Carbon* **2013**, *58*, 99−106.
(17) Tao, X.; Zhang, J.; Xia, Y.; Huang, H.; Du, J.; Xiao, H.; Zhang, W.; Gan, Y. Bio-Inspired Fabrication of Carbon Nanotiles for High Performance Cathode of Li-S Batteries. *J. Mater. Chem. A* **2014**, *2*, 2290−2296.
(18) Ye, H.; Yin, Y.-X.; Xin, S.; Guo, Y.-G. Tuning the Porous Structure of Carbon Hosts for Loading Sulfur Toward Long Lifespan Cathode Materials for Li-S Batteries. *J. Mater. Chem. A* **2013**, *1*, 6602−6608.
(19) Yin, L.; Wang, J.; Yu, X.; Monroe, C. W.; NuLi, Y.; Yang, J. Dual-Mode Sulfur-Based Cathode Materials for Rechargeable Li−S Batteries. *Chem. Commun.* **2012**, *63*, 7868−7870.
(20) Li, W.; Zheng, G.; Yang, Y.; Seh, Z. W.; Liu, N.; Cui, Y. High-Performance Hollow Sulfur Nanostructured Battery Cathode through a Scalable, Room Temperature, One-Step, Bottom-Up Approach. *Proc. Natl. Acad. Sci. U. S. A.* **2013**, *110*, 7148−7153.
(21) Jayaprakash, N.; Shen, J.; Moganty, S. S.; Corona, A.; Archer, L. A. Porous Hollow Carbon@Sulfur Composites for High-Power Lithium−Sulfur Batteries. *Angew. Chem., Int. Ed.* **2011**, *50*, 5904−5908.
(22) Zhang, C.; Wu, H. B.; Yuan, C.; Guo, Z.; Lou, X. W. Confining Sulfur in Double-Shelled Hollow Carbon Spheres for Lithium−Sulfur Batteries. *Angew. Chem., Int. Ed.* **2012**, *51*, 9592−9595.
(23) Wei Seh, Z.; Li, W.; Cha, J. J.; Zheng, G.; Yang, Y.; McDowell, M. T.; Hsu, P.-C.; Cui, Y. Sulphur−TiO_2 Yolk−Shell Nanoarchitecture with Internal Void space for Long-Cycle Lithium−Sulphur Batteries. *Nat. Commun.* **2013**, *4*, 1331−1337.
(24) Xu, H.; Deng, Y.; Shi, Z.; Qian, Y.; Meng, Y.; Chen, G. Graphene-Encapsulated Sulfur (GES) Composites with a Core-Shell Structure as Superior Cathode Materials for Lithium-Sulfur Batteries. *J. Mater. Chem. A* **2013**, *1*, 15142−15149.
(25) Miao, L.-X.; Wang, W.-K.; Wang, A.-B.; Yuan, K.-G.; Yang, Y.-S. A High Sulfur Content Composite with Core-Shell Structure as Cathode Material for Li-S Batteries. *J. Mater. Chem. A* **2013**, *1*, 11659−11664.
(26) Chung, S.-H.; Manthiram, A. A Hierarchical Carbonized Paper with Controllable Thickness as a Modulable Interlayer System for High Performance Li-S Batteries. *Chem. Commun.* **2014**, *50*, 4184−4187.
(27) Wang, X.; Wang, Z.; Chen, L. Reduced Graphene Oxide Film as a Shuttle-Inhibiting Interlayer in a Lithium−Sulfur Battery. *J. Power Sources* **2013**, *242*, 65−69.
(28) Su, Y.-S.; Manthiram, A. Lithium−Sulphur Batteries with a Microporous Carbon Paper as a Bifunctional Interlayer. *Nat. Commun.* **2012**, *3*, 1166−1172.
(29) Jeong, T.-G.; Moon, Y. H.; Chun, H.-H.; Kim, H. S.; Cho, B. W.; Kim, Y.-T. Free Standing Acetylene Black Mesh to Capture Dissolved Polysulfide in Lithium Sulfur batteries. *Chem. Commun.* **2013**, *49*, 11107−11109.
(30) Zu, C.; Su, Y.-S.; Fu, Y.; Manthiram, A. Improved Lithium-Sulfur Cells with a Treated Carbon Paper Interlayer. *Phys. Chem. Chem. Phys.* **2013**, *15*, 2291−2297.
(31) Woo, J.-J.; Zhang, Z.; Amine, K. Separator/Electrode Assembly Based on Thermally Stable Polymer for Safe Lithium-Ion Batteries. *Adv. Energy Mater.* **2013**, *5*, 1301208−1301212.
(32) Yan, L.; Li, Y. S.; Xiang, C. B. Preparation of Poly (Vinylidene Fluoride)(pvdf) ultrafiltration Membrane Modified by Nano-Sized Alumina (Al_2O_3) and Its Antifouling Research. *Polymer* **2005**, *46*, 7701−7706.
(33) Jayaprakash, N.; Shen, J.; Moganty, S. S.; Corona, A.; Archer, L. A. Porous Hollow Carbon@ Sulfur Composites for High-Power Lithium−Sulfur Batteries. *Angew. Chem.* **2011**, *123*, 6026−6030.
(34) Wu, F.; Chen, J.; Chen, R.; Wu, S.; Li, L.; Chen, S.; Zhao, T. Sulfur/Polythiophene with a Core/Shell Structure: Synthesis and Electrochemical Properties of the Cathode for Rechargeable Lithium Batteries. *J. Phys. Chem. C* **2011**, *115*, 6057−6063.
(35) Yu, L.-Y.; Xu, Z.-L.; Shen, H.-M.; Yang, H. Preparation and Characterization of PVDF−SiO_2 Composite Hollow Fiber UF Membrane by Sol−Gel Method. *J. Membr. Sci.* **2009**, *337*, 257−265.
(36) Cao, X.; Ma, J.; Shi, X.; Ren, Z. Effect of TiO_2 Nanoparticle Size on the Performance of PVDF Membrane. *Appl. Surf. Sci.* **2006**, *253*, 2003−2010.
(37) Xie, J.; Yang, J.; Zhou, X.; Zou, Y.; Tang, J.; Wang, S.; Chen, F. Preparation of Three-Dimensional Hybrid Nanostructure-Encapsulated Sulfur Cathode for High-Rate Lithium Sulfur Batteries. *J. Power Sources* **2014**, *253*, 55−63.
(38) Soresi, B.; Quartarone, E.; Mustarelli, P.; Magistris, A.; Chiodelli, G. PVDF and P (VDF-HFP)-Based Proton Exchange Membranes. *Solid State Ionics* **2004**, *166*, 383−389.
(39) Ross, G.; Watts, J.; Hill, M.; Morrissey, P. Surface Modification of Poly (Vinylidene Fluoride) by Alkaline Treatment1. The Degradation Mechanism. *Polymer* **2000**, *41*, 1685−1696.
(40) Abdel-Hamid, H. M. Effect of Electron Beam Irradiation on Polypropylene Films-Dielectric and FT-IR Studies. *Solid-State Electron.* **2005**, *4*, 1163−1167.
(41) Boccaccio, T.; Bottino, A.; Capannelli, G.; Piaggio, P. Characterization of PVDF Membranes by Vibrational Spectroscopy. *J. Membr. Sci.* **2002**, *210*, 315−329.
(42) Bormashenko, Y.; Pogreb, R.; Stanevsky, O.; Bormashenko, E. Vibrational Spectrum of PVDF and Its Interpretation. *Polym. Test.* **2004**, *23*, 791−796.
(43) Yuan, Z.; Dan-Li, X. Porous PVDF/TPU Blends Asymmetric Hollow Fiber Membranes Prepared with the Use of Hydrophilic Additive PVP (K30). *Desalination* **2008**, *223*, 438−447.
(44) Kise, H.; Ogata, H. Phase Transfer Catalysis in Dehydrofluorination of Poly (Vinylidene Fluoride) by Aqueous Sodium Hydroxide Solutions. *J. Polym. Sci., Part A: Polym. Chem.* **1983**, *21*, 3443−3451.
(45) Yuan, Z.; Dan-Li, X. Porous PVDF/TPU Blends Asymmetric Hollow Fiber Membranes Prepared with the Use of Hydrophilic Sdditive PVP (K30). *Desalination* **2008**, *223*, 438−447.
(46) Sairiam, S.; Loh, C. H.; Wang, R.; Jiraratananon, R. Surface Modification of PVDF Hollow Fiber Membrane to Enhance Hydrophobicity Using Organosilanes. *J. Appl. Polym. Sci.* **2013**, *130*, 610−621.
(47) Liang, S.; Kang, Y.; Tiraferri, A.; Giannelis, E. P.; Huang, X.; Elimelech, M. Highly hydrophilic polyvinylidene fluoride (PVDF) ultrafiltration membranes via postfabrication grafting of surface-tailored silica nanoparticles. *ACS Appl. Mater. Interfaces* **2013**, *5*, 6694−6703.
(48) Xiao, L.; Cao, Y.; Xiao, J.; Schwenzer, B.; Engelhard, M. H.; Saraf, L. V.; Nie, Z.; Exarhos, G. J.; Liu, J. Molecular structures of polymer/sulfur composites for lithium-sulfur batteries with long cycle life. *J. Mater. Chem. A* **2013**, *1*, 9517−9526.